



Development of Heterogenous Catalyst from Cocoa Pods Husk and Sawdust

¹Yakubu Yerima and ^{1*}Idongesit Helen Nsidibe-Obong

^ayerima.yakubu@iuokada.edu.ng; ^bidongesit.helen@iuokada.edu.ng

¹Department of Chemical Engineering, College of Engineering, Igbinedion University, Okada, Edo State, Nigeria

*Corresponding Author: Idongesit Helen Nsidibe-Obong; idongesit.helen@iuokada.edu.ng

Manuscript History

Received: 12/02/2026

Revised: 25/03/2026

Accepted: 15/04/2026

Published: 20/04/2026

<https://doi.org/10.5281/zenodo.19957557>

Abstract: The increasing need for sustainable and environmentally friendly catalytic materials has led to the investigation of agricultural waste as alternative feedstock. This study centered on creating a heterogeneous catalyst sourced from cocoa pod husk and sawdust, which are two plentiful agro-industrial byproducts. The precursor went through series of unit operations and thermal treatment thereby leading to its activation into an heterogenous catalyst and was further characterized. The developed heterogenous catalyst was characterized using Fourier Transform Infrared Spectroscopy (FT-IR), Scanning Electron Microscopy/Energy Dispersive X-ray (SEM/EDX), Brunauer Emmett Teller (BET), Thermogravimetric Analysis (TGA) and X-ray Diffraction (XRD). The FT-IR analysis indicated the presence of hydroxyl groups, hydrocarbon and halo compounds. The SEM/EDX assessed the surface structure and elemental composition; it showed majorly the presence of alkali metals (potassium 55.02%, sodium 0.22%) and alkaline earth metals (calcium 28.19%, magnesium 6.38%). BET analysis indicated that the pore diameter was 2.072nm, pore volume 0.191cc/g and surface area 395.047m²/g. TGA analysis showed the thermal stability; with an ideal optimal temperature of 480 °C. XRD analysis indicated the presence of muscovite, showing that the heterogenous catalyst was highly crystalline. A comparative study was conducted on the biocatalyst by examining its elemental composition and functional groups in relation to other biocatalysts; the findings indicated that it is appropriate for biodiesel production due to its similarity in functional groups and elemental composition. This research highlights the potential of converting cocoa pod husk and sawdust into low-cost, renewable materials for catalyst production, thereby supporting green chemistry and waste-to-resource initiatives.

Keywords: Heterogeneous Catalyst, Cocoa Pod Husks, Sawdust, Calcination, Biodiesel

INTRODUCTION

In various chemical industries such as pharmaceuticals, agricultural, food and beverages, the need and application of heterogeneous catalysts have increased due to its advantages (such as sustainability, renewability, ability to work with complex substrates, mild reaction condition) compared to chemical catalysts (Patil & Rathod, 2021). Scientists over the years have been researching on the production of new biocatalysts to increase the range at which these biocatalysts are applied in industries (Shetty *et al.*, 2023; Usami, 2024). These researchers either modify the existing enzymes or discover new enzymes to develop biocatalysts. Waste biomass (biowastes) from agricultural products have recently been burned as traditional fuel which results to air pollution. As a result of this, the conversion of these bio-wastes into high value products like biocatalyst is very vital. Biocatalysts are

biodegradable in nature, and their production requires renewable raw materials. Biocatalysts are driving towards creating more efficient and environmentally friendly manufacturing processes. In the coming decades, the discovery of improved biocatalysts will enhance improvements in many industrial processes (Pandeeti *et al.*, 2019). The use of these biocatalysts in the transformation of chemicals is referred to as biocatalysis.

The use of biowaste for the production and development of biocatalysts aids at reducing cost and increases the recycling of waste in the environment. Plant biomass (such as rice husk, cocoa pod husk, saw dust, plantain peels etc.) is the most abundant and sustainable source of biomass on earth.

One of the key reasons of using plant biomass for the development of biocatalyst is that its availability is proportional to the production of food crops as additional land for cultivation is not required. Hence, it provides an economical and environmental-friendly alternative to other substrates used in various industries application (Gronenberg *et al.*, 2013; Usami, 2024). Cocoa pod (*Theobroma cacao*) husk is gotten from cocoa after the cocoa seeds have been removed from the fruit. About 30% of cocoa, especially cocoa nibs, are used as the primary ingredient for production of chocolate; while 70% is either used as animal feed or disposed of as waste. The by-product from cocoa includes cocoa pod husk, cocoa shell, cocoa butter, cocoa cake, cocoa powder, pulp and sweating (Anaraga *et al.*, 2024). Sawdust is a biowaste material from the processing of wood. These wastes are usually disposed of thereby resulting to environmental pollution. There has been effort placed to recycle these materials into useful industrial products to enhance environmental waste management. The development of biocatalyst from cocoa pod husk and sawdust will require the combination of different composition of catalyst from cocoa pod husk and sawdust due to the presence of proteins, cellulose and cellulose binding molecule proteins in both biowaste. While studies have shown that cocoa pod husk can be used to produce biocatalysts for biodiesel production with conversion rate of up to 98% (Laskar *et al.*, 2020), there is need for further research on scaling up the production process to meet industrial demands and improve the stability and usability of the catalyst to make it more economically viable.

MATERIALS AND METHODS

2.1 Materials

One kilogram (1kg) of cocoa pod husk was collected from a farm in Okada, Ovia Northeast LGA, Edo State, Nigeria. Additionally, five hundred grams (500g) of sawdust was obtained from a sawmill in the same area. Cocoa pod husk and sawdust served as the lignocellulosic sources for the heterogeneous catalyst. There was no use of extra catalyst support or binder. Distilled water was utilized for washing. Analytical grade reagents and chemicals were used for the study.

2.2 Preparation of Precursor

The CPH and sawdust used in this study were treated separately before calcination. The cocoa pod husks were thoroughly washed with distilled water to eliminate any residues as well as dirt. This cleaning procedure was performed to facilitate the drying process and prevent contamination of the heterogeneous catalyst. The washed cocoa pod husks and sawdust were sun-dried for 72 hours and 12 hours, respectively, until the moisture content was significantly reduced. The cocoa pod husks were further oven-dried at 100°C until a constant weight was observed. The dried cocoa pod husks were placed into a mortar to be crushed to a size suitable for blending. After this, they were transferred to an industrial blender until a particle size of approximately 5mm to 50mm was achieved. Both the cocoa pod husk and sawdust samples were sieved using an 80-mesh size sieve to ensure uniform particle size, and then they were stored in an airtight container.

2.3 Preparation and Characterization of Catalyst

The stored CPH and sawdust (50:50) were transferred to a porcelain crucible and calcined in a muffle furnace at pods temperature of 800°C for 4hours until they completely turned ash according to Falowo *et al* (2022). When CPH and sawdust are calcined, their constituents become concentrated and form active catalytic sites. The catalyst was allowed to cool and immediately stored in an airtight container to avoid moisture absorption. The synthesized catalyst was characterized according to Falowo *et al* (2022)

RESULTS AND DISCUSSION

3.1 Fourier Transform Infrared Spectroscopy (FT-IR)

This chapter shows the result of the characterization analysis of the precursor and calcined sample (biocatalyst) of CPH-Sawdust. The following characterization: FT-IR, SEM-EDX, TGA, BET and XRD were carried out.

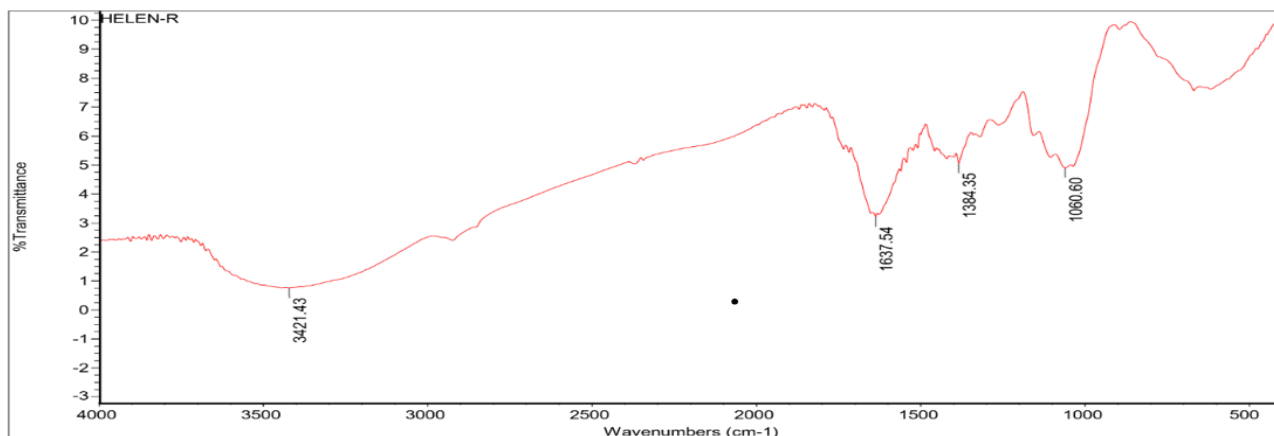


Fig. 1 FT-IR Analysis of Catalyst Precursor

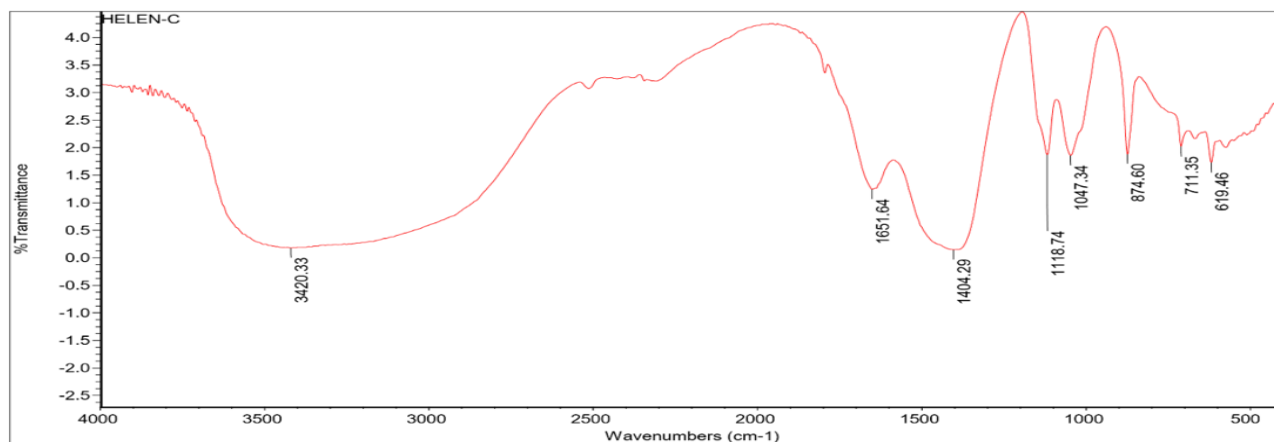


Fig. 2 FT-IR Analysis of Heterogenous Biocatalyst

The FT-IR analysis was done on the precursor and heterogenous biocatalyst to study the different composition of functional groups. In the spectrum of the precursor as shown in Fig. 1, the broad peak located at 3421.43 cm⁻¹ wavelength indicated the O-H stretching vibration (i.e. hydroxyl group) present in alcoholic and phenolic compounds from the CPH-Sawdust. These functional groups are responsible for reducing metal ions and stabilizing synthesized nanoparticles to prevent agglomeration. The peak located at 1637.54cm⁻¹ indicated C=C stretching for alkene which can participate in adsorption. The peak at 1384.35cm⁻¹ denoted a C-H bending vibration indicating the presence of organic compounds (such as lignin and cellulose). The peak at 1060.60 showed a C-O stretching vibration in ethers responsible for binding and reactivity. For the heterogenous biocatalyst spectrum as shown in Fig.2, the broad peak with wavelength of 3420.33cm⁻¹ indicated O-H stretching vibration. The peak at 1651.64cm⁻¹ showed C=C stretching vibration indicating the presence of alkene. The peak at 1404.29cm⁻¹ indicated C-H bending vibration. The peak located at 1118.74cm⁻¹ showed C-O stretching vibrations and 1047.34cm⁻¹ showed C-O-C stretching vibrations. The peak at 874.60 cm⁻¹ corresponded to the Metal-O vibration indicating the presence of oxides of metals. The peak at 711.35cm⁻¹ and 619.46cm⁻¹ indicated C-Cl stretching vibrations.

3.2 Scanning Electron Microscopy/Energy Dispersive X-ray Spectroscopy (SEM-EDX)

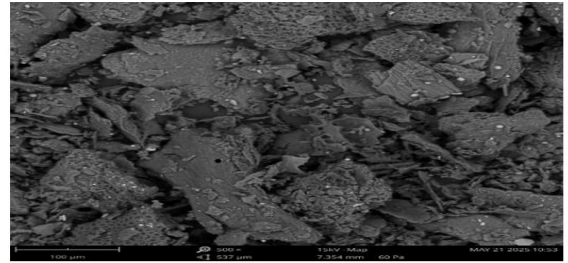
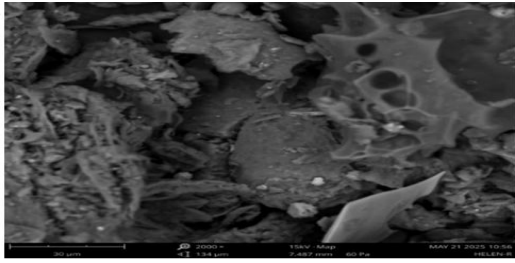


Fig. 3 SEM/EDX images of Catalyst Precursor

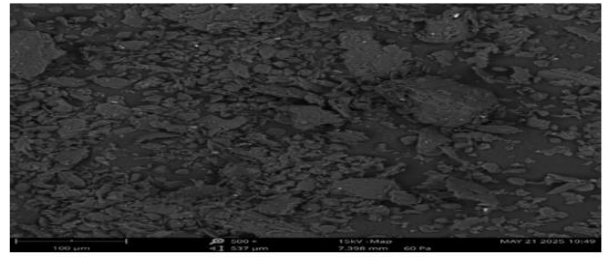
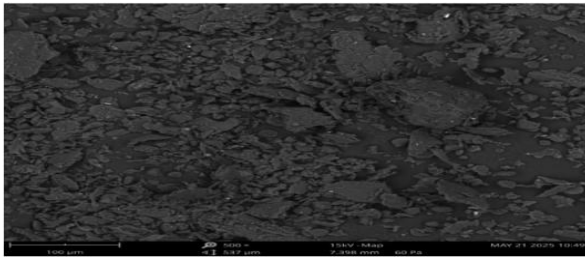


Fig. 4 SEM-EDX Images of Heterogenous Biocatalyst

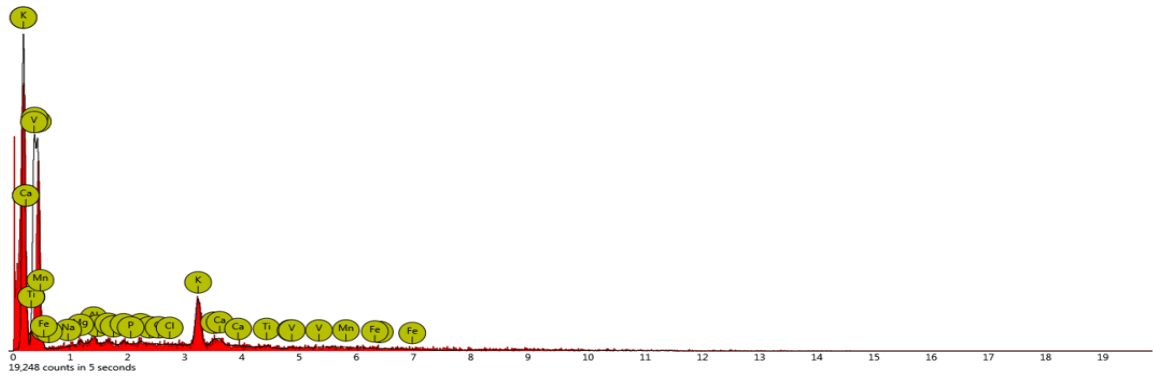


Fig. 5 SEM/EDX Spectra of Precursor

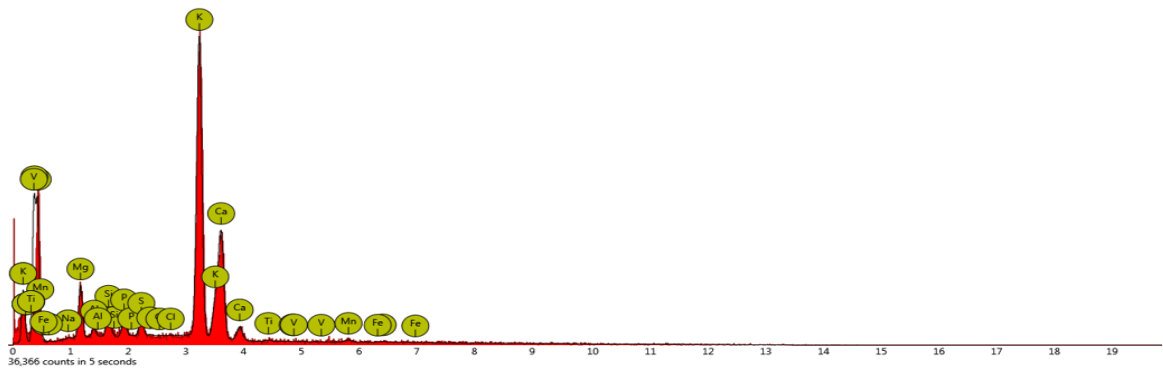


Fig. 6 SEM/EDX Spectra of Heterogenous Biocatalyst

The images obtained at a magnitude of 500x consisted of irregular, flake-like and granular particles as shown in Fig. 3 and Fig. 4 for the precursor and heterogenous biocatalyst respectively. The SEM showed a heterogenous distribution of particle sizes between the range of 5µm and 100µm. The Fig. 4 is the calcined sample (i.e. heterogenous biocatalyst) which showed an increased porosity. The surface texture appears rough and porous, which is very common for biomass-derived materials after calcination. It is evident that the weight composition of some elements increased or decreased after calcination which means that the calcination process helped in the efficiency of some elements in the precursor. Potassium (K) is seen to be the most dominant element in the heterogenous biocatalyst as shown in Fig. 6, followed by calcium, magnesium (Mg), silicon (Si), phosphorus (P), Sulphur (S), manganese (Mn), aluminum (Al), titanium (Ti) and sodium (Na). These elements through calcination process are converted into their oxide forms. These elements gave the heterogenous biocatalyst a high catalytic activity in biodiesel production; other biomass-derived catalyst have these same elements present with potassium as the key element (Etim & Musonge, 2024).

3.3 Braeuer-Emmett-Teller (BET)

BET analysis was carried out on both the precursor and heterogenous biocatalyst to analyze the pore diameter, surface area and pore volume. Fig. 8 and Fig. 10 showed the summary of the result for the precursor and heterogenous catalyst respectively using different methods but the method prioritized in this discussion is the BJH because it can measure mesopores (2nm-50nm). In Fig. 7 there was a decrease in the surface area, pore volumes and pore diameter when compared to Fig. 9. The surface areas of the precursor and heterogenous catalyst were 454.876m²/g and 395.047m²/g, their pore volumes were 0.221cc/g and 0.191cc/g while their pore diameter were 2.093nm and 2.072nm respectively. The decrease in surface area, pore volume and diameter was as a result of high temperature calcination and duration (Falowo & Biteku, 2022); hence controlled temperature has a positive effect on the activity of the catalyst (Sui et al., 2024).

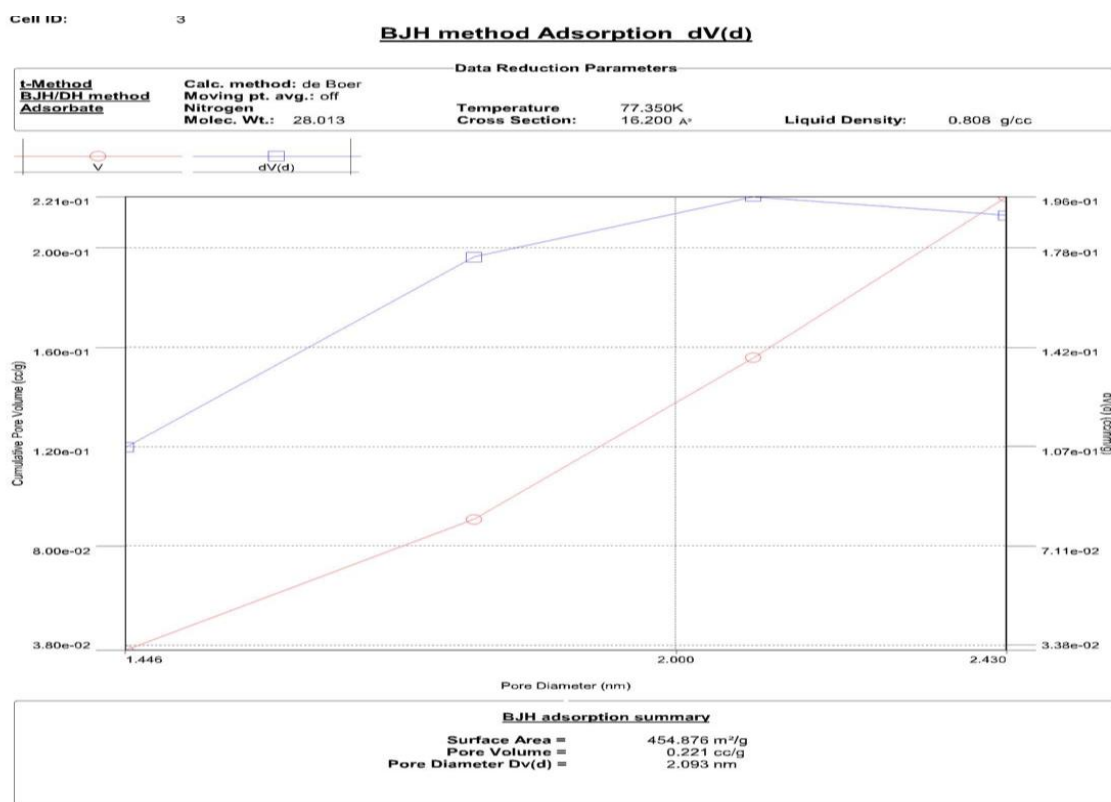


Fig. 7 BET Analysis for Catalyst Precursor (CPH-Sawdust)

Analysis		Report	
Operator:	Abdulrahman Abdulkareem	Date:	2025/05/19
Sample ID:	Helen - R	Filename:	Helen - R.qps
Sample Desc:		Comment:	
Sample weight:	0.3 g	Sample Volume:	1 cc
Outgas Time:	3.0 hrs	OutgasTemp:	250.0 C
Analysis gas:	Nitrogen	Bath Temp:	273.0 K
Press. Tolerance:	0.100/0.100 (ads/des)	Equil time:	60/60 sec (ads/des)
Analysis Time:	365.6 min	End of run:	2025/05/19 11:15:09
Cell ID:	3	Equil timeout:	240/240 sec (ads/des)
		Instrument:	Nova Station C

Area-Volume Summary

Data Reduction Parameters Data

t-Method	Thermal Transpiration: off	Eff. mol. diameter (D): 3.54 Å	Eff. cell stem diam. (d): 4.0000 mm
BJH/DH method	Calc. method: de Boer		
DR method	Moving pt. avg.: off		
HK method	Affinity coefficient (β): 0.3300		
SF method	Tabulated data interval: 1		
DFT method	Tabulated data interval: 1		
	Calc. Model: N2 at 77 K on carbon (slit pore, NLDFT equilibrium model)		
	Rel. press. range: 0.0000 - 1.0000		Moving pt. avg: off
Adsorbate	Nitrogen	Temperature: 77.350K	Liquid Density: 0.808 g/cc
	Molec. Wt.: 28.013	Cross Section: 16.200 Å²	SuperCritical. K.: 1.000
	Critical Temp.: 126.200 K	Critical Press.: 33.500 atm	
Adsorbent	Carbon		
	DR. Exp (n): 2.000		

Surface Area Data

SinglePoint BET.....	2.552e+02 m²/g
MultiPoint BET.....	3.570e+02 m²/g
Langmuir surface area.....	1.012e+03 m²/g
BJH method cumulative adsorption surface area.....	4.549e+02 m²/g
DH method cumulative adsorption surface area.....	4.846e+02 m²/g
t-method external surface area.....	3.570e+02 m²/g
DR method micropore area.....	4.173e+02 m²/g
DFT cumulative surface area.....	1.023e+02 m²/g

Pore Volume Data

BJH method cumulative adsorption pore volume.....	2.206e-01 cc/g
DH method cumulative adsorption pore volume.....	2.260e-01 cc/g
DR method micropore volume.....	1.483e-01 cc/g
HK method micropore volume.....	7.077e-02 cc/g
SF method micropore volume.....	2.074e-02 cc/g
DFT method cumulative pore volume.....	1.205e-01 cc/g

Pore Size Data

BJH method adsorption pore Diameter (Mode Dv(d)).....	2.093e+00 nm
DH method adsorption pore Diameter (Mode Dv(d)).....	2.093e+00 nm
DR method micropore Pore width.....	5.634e+00 nm
DA method pore Diameter (Mode).....	2.780e+00 nm
HK method pore Diameter (Mode).....	3.675e-01 nm
SF method pore Diameter (Mode).....	4.523e-01 nm
DFT pore Diameter (Mode).....	2.647e+00 nm

Fig. 8 BET Analysis Summary for Precursor (CPH-Sawdust)

BJH method Adsorption dV(d)

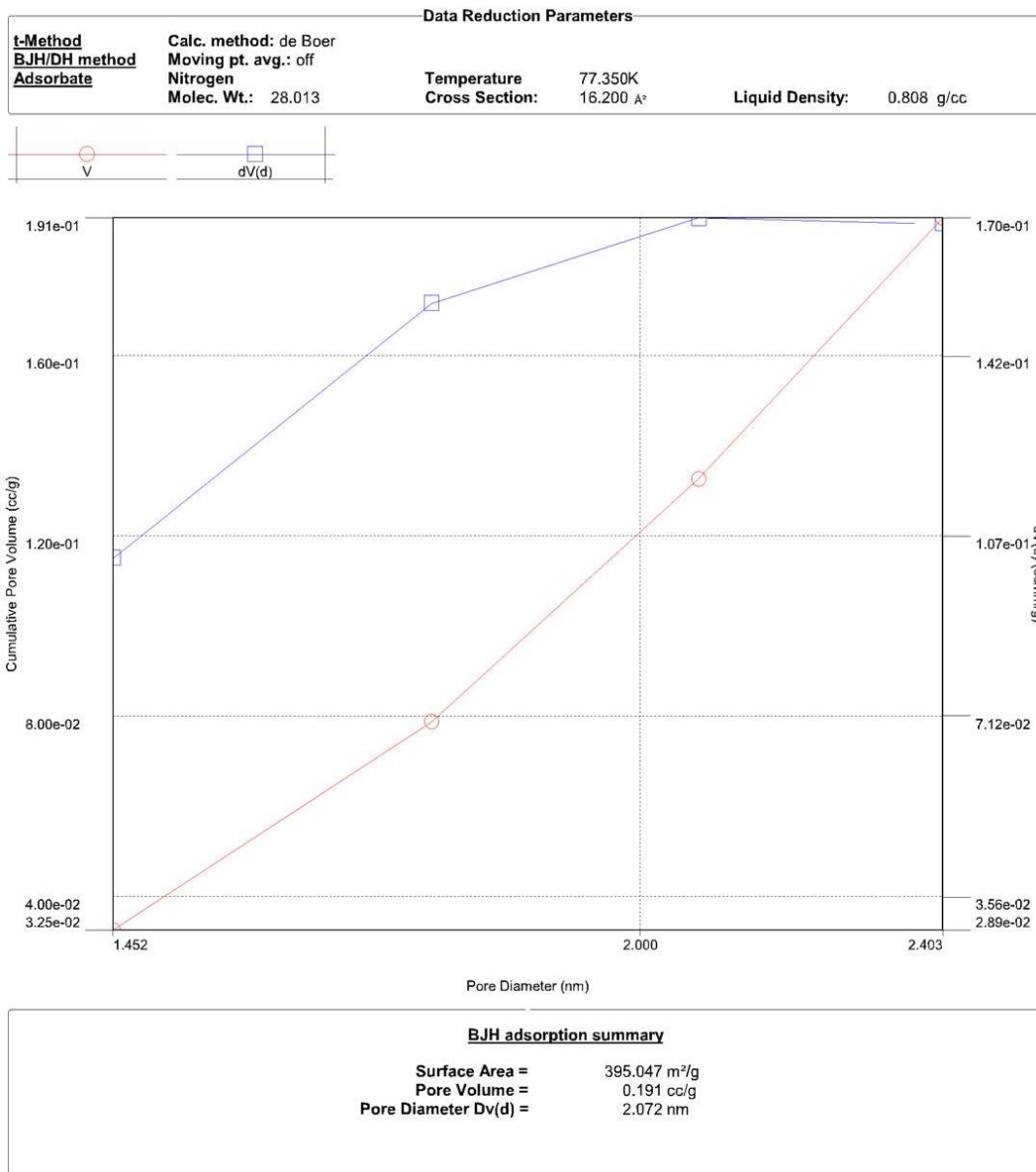


Fig. 9 BET Analysis for Heterogenous Biocatalyst

Analysis	Abdulrahman Abdulkareem	Date: 2025/05/19	Report	Operator: Abdulrahman Abdulkareem	Date: 2025/05/19
Operator:	Helen - C	Filename:	Helen - C.qps		
Sample ID:	Helen - C	Comment:			
Sample Desc:		Sample Volume:	1 cc		
Sample weight:	0.35 g	OutgasTemp:	250.0 C		
Outgas Time:	3.0 hrs	Bath Temp:	273.0 K		
Analysis gas:	Nitrogen	Equil time:	60/60 sec (ads/des)		
Press. Tolerance:	0.100/0.100 (ads/des)	End of run:	2025/05/19 10:03:00		
Analysis Time:	77.4 min	Equil timeout:	240/240 sec (ads/des)		
Cell ID:	3	Instrument:	Nova Station C		

Area-Volume Summary

Data Reduction Parameters Data

t-Method	Thermal Transpiration: off	Eff. mol. diameter (D): 3.54 Å	Eff. cell stem diam. (d): 4.0000 mm
BJH/DH method	Calc. method: de Boer		
DR method	Moving pt. avg.: off		
HK method	Affinity coefficient (β): 0.3300		
SF method	Tabulated data interval: 1		
DFT method	Tabulated data interval: 1		
	Calc. Model: N2 at 77 K on carbon (slit pore, NLDFT equilibrium model)		
Adsorbate	Nitrogen	Temperature: 77.350K	Moving pt. avg: off
	Molec. Wt.: 28.013	Cross Section: 16.200 Å²	Liquid Density: 0.808 g/cc
Adsorbent	Carbon	Critical Press.: 33.500 atm	SuperCritical. K.: 1.000
	DR. Exp (n): 2.000		

Surface Area Data

SinglePoint BET.....	2.284e+02 m²/g
MultiPoint BET.....	3.099e+02 m²/g
Langmuir surface area.....	7.961e+02 m²/g
BJH method cumulative adsorption surface area.....	3.950e+02 m²/g
DH method cumulative adsorption surface area.....	4.199e+02 m²/g
t-method external surface area.....	3.099e+02 m²/g
DR method micropore area.....	3.756e+02 m²/g
DFT cumulative surface area.....	9.400e+01 m²/g

Pore Volume Data

BJH method cumulative adsorption pore volume.....	1.906e-01 cc/g
DH method cumulative adsorption pore volume.....	1.949e-01 cc/g
DR method micropore volume.....	1.335e-01 cc/g
HK method micropore volume.....	6.561e-02 cc/g
SF method micropore volume.....	2.097e-02 cc/g
DFT method cumulative pore volume.....	1.088e-01 cc/g

Pore Size Data

BJH method adsorption pore Diameter (Mode Dv(d)).....	2.072e+00 nm
DH method adsorption pore Diameter (Mode Dv(d)).....	2.072e+00 nm
DR method micropore Pore width.....	5.555e+00 nm
DA method pore Diameter (Mode).....	2.740e+00 nm
HK method pore Diameter (Mode).....	3.675e-01 nm
SF method pore Diameter (Mode).....	4.523e-01 nm
DFT pore Diameter (Mode).....	2.647e+00 nm

Fig. 10 BET Analysis Summary for Heterogenous Biocatalyst

3.4 Thermogravimetric Analysis (TGA)

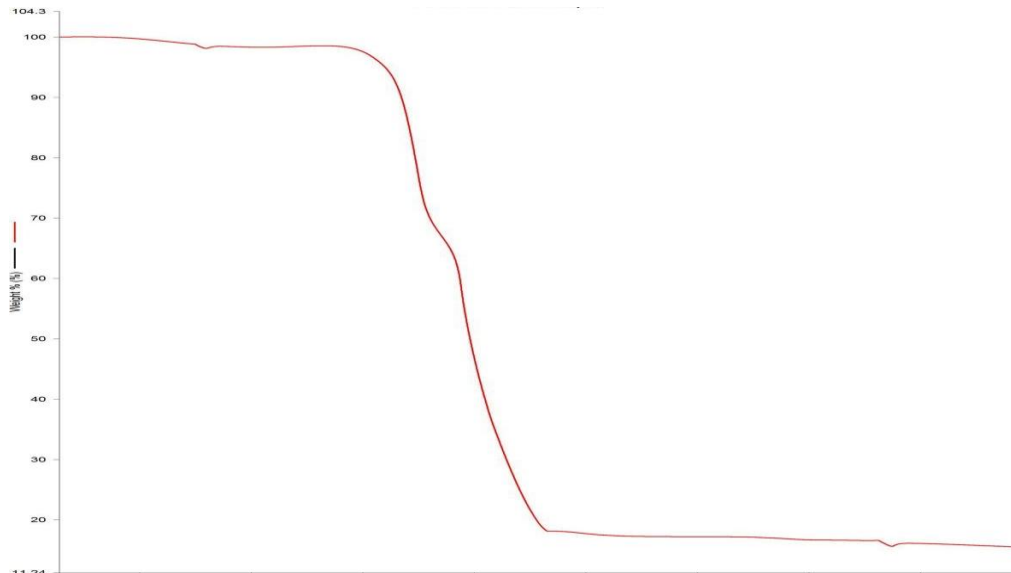


Fig. 11 TGA of Catalyst Precursor (CPH-Sawdust)

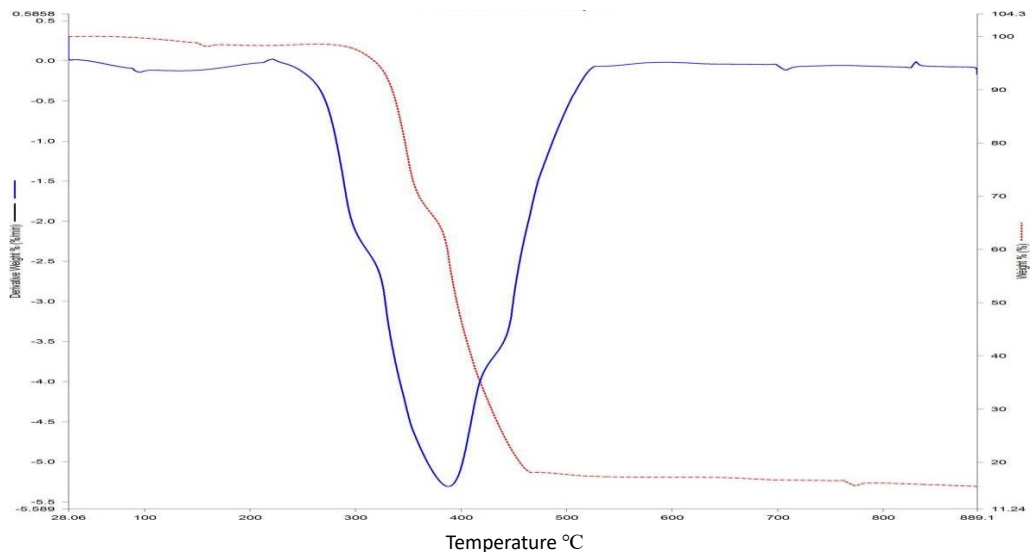


Fig. 12 TGA of Catalyst Precursor (CPH-Sawdust)

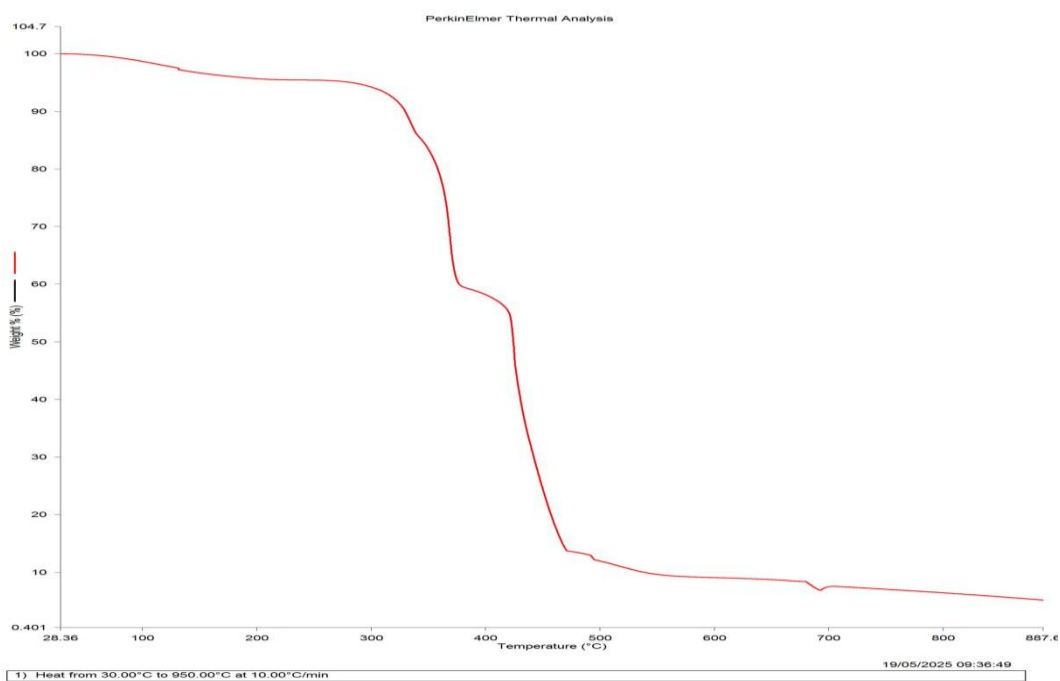


Fig. 13 TGA Analysis for the Heterogenous Catalyst

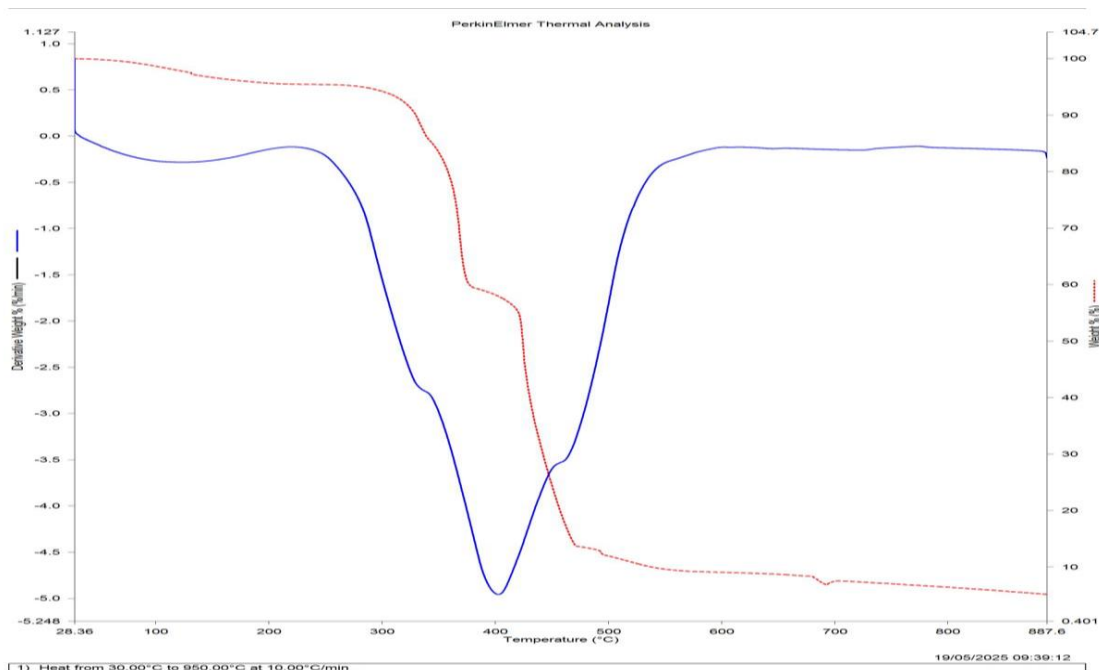


Fig. 14 TGA Analysis for the Heterogenous Catalyst

The TGA analysis of the precursor and heterogenous biocatalyst are shown in Fig. 11 and Fig. 13 respectively. The plot of the heterogenous biocatalyst (Fig. 13) showed a weight loss of 2% between 0°C and 150°C which was as a result of removal of moisture. The additional decrease in the weight of the catalyst may likely be as a result of organic decomposition. The large weight loss of the heterogenous catalyst as shown in Fig. 13 correlated with the result from BET and SEM/EDX which showed the decrease in surface area and elemental composition; this was due to high temperature during calcination (Kasi *et al.*, 2025). From the plot in Fig. 13, the ideal optimal temperature for calcination was 480°C at a lesser duration.

3.5 X-Ray Diffraction (XRD)

The XRD analysis in Fig. 15 and Table-1 indicated the presence of 71% muscovite ($KAl_2(AlSi_3O_{10})(OH)_2$), a layered silicate. It also detected the presence of graphite (13%), 9.8% of cristobalite which is a high-temperature polymorph of silica; this signified it has undergone significant thermal treatment and 5.4% silvialite which is a lesser silicate phase, are also detected. The small portion of urea (1%) implies complete decomposition, which is characteristic of effective calcination. Similarly, in Fig. 16 and Table-2 the percentage of muscovite, graphite, cristobalite, silvialite and urea in the heterogenous catalyst are 67.3%, 3.37%, 2.52%, 21% and 5.7% respectively. The presence of potassium in muscovite correlated with its presence in the SEM/EDX analysis. The CPH-Sawdust heterogenous biocatalyst was highly crystalline due to the presence of large amount of muscovite and graphite, including cristobalite, silvialite and urea which make it suitable as a catalyst (Wang *et al.*, 2025).

Table-1 XRD Analysis for Catalyst Precursor

Dataset / Weight Fraction, wt%	Value, Unit	Urea, syn	Graphite	Muscovite	Cristobalite	Silvialite
HELEN_R_20250522_090033_G 0		1(4)	13.1(5)	71(3)	9.8(4)	5.4(2)

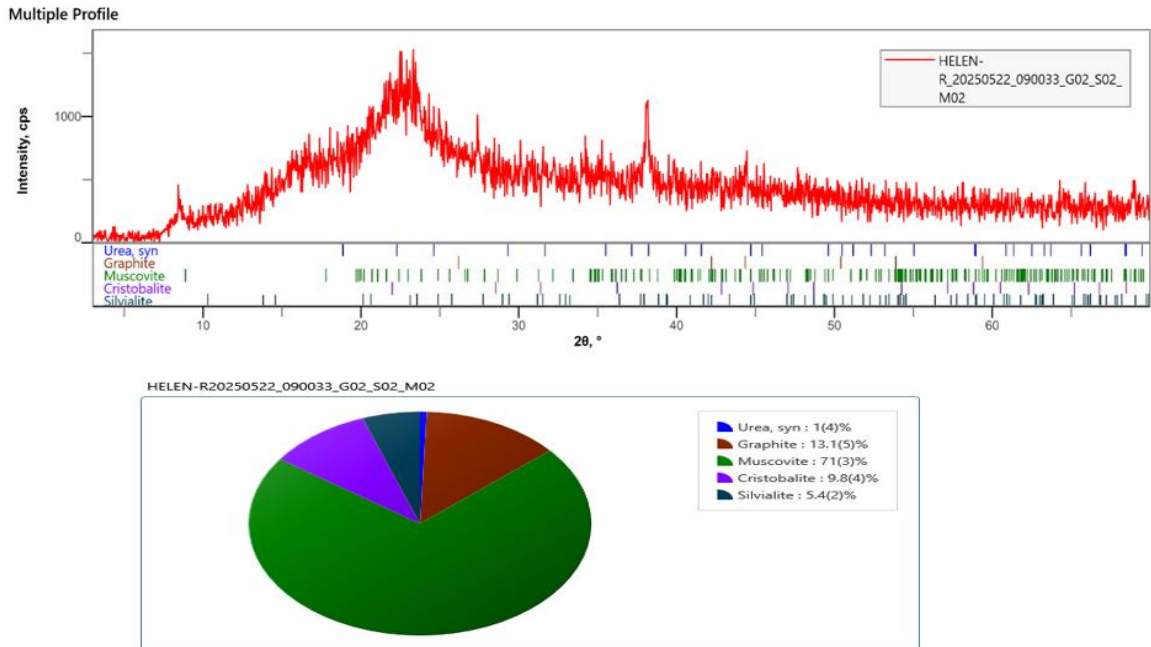


Fig. 15 XRD of Catalyst Precursor (CPH-Sawdust)

Table-2 XRD Analysis for the Heterogenous Catalyst

Dataset / Weight Fractio Value,	Muscovit	Urea,	Cristobalite	Graphit	Silivalit
HELEN_C_20250522_090033_G 0	67.3(12)	5.7(2)	2.52(9)	3.37(13)	21.0(8)

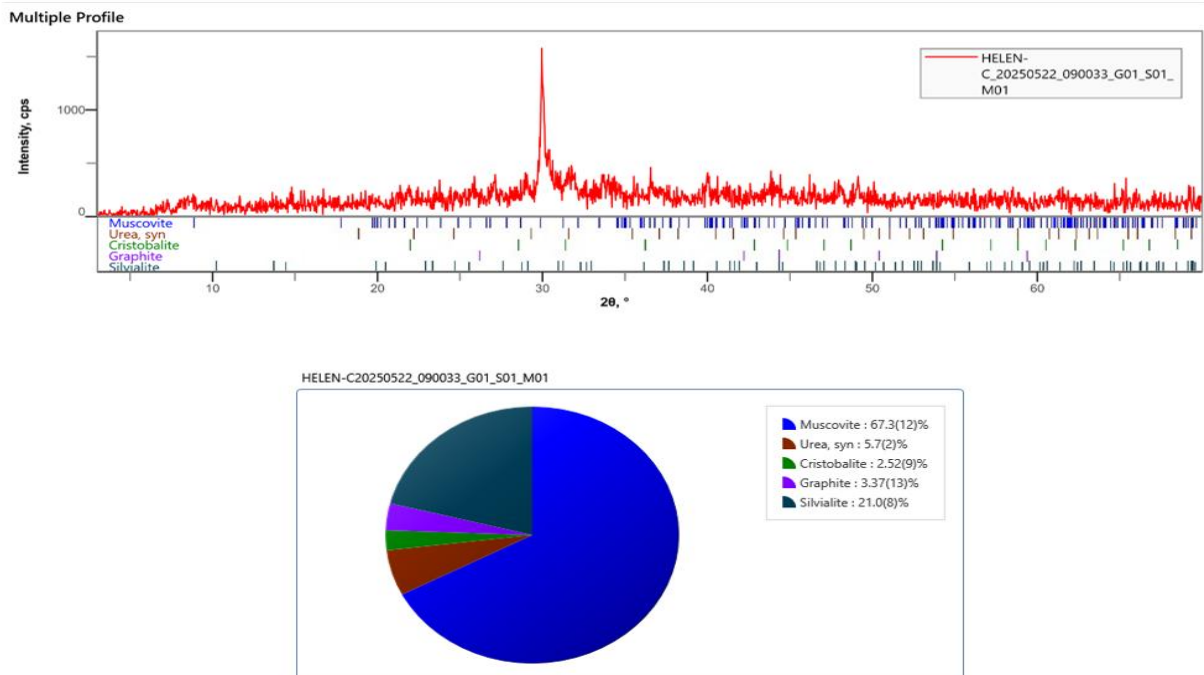


Fig. 16 XRD Analysis for the Heterogenous Catalyst

3.6. Comparative Analysis of Heterogenous Biocatalyst

The CPH-Sawdust heterogenous biocatalyst was compared with other biocatalysts and the results are shown in Table-3.

Table-3 Comparative Analysis of the Elemental Composition of Heterogenous Catalyst

Source of Catalyst	Metallic Oxides Composition (%)													Biodiesel Yield (%)
	Na	K	Ca	Mg	Mn	Fe	Zn	Al	P	Si	Cl	C	O	
Mangifera indica peel (Laskar <i>et al.</i> , 2020)	0.25	43.89	9.44	3.07	-	0.46	-	-	4.21	2.61	-	2.38	32.54	98
Sweet potato leaves (Eldiehy <i>et al.</i> , 2022)	0.70	65.45	18.02	4.63	-	0.88	-	0.94	-	3.54	4.12	-	-	98.75
Cocoa pod husk + plantain peel (Olatundun <i>et al.</i> , 2020)	0.0	51.94	0.0	2.05	-	0.0	-	-	1.04	1.01	2.77	-	40.93	98.98
Cocoa pod husk (Betiku <i>et al.</i> , 2017)	-	59.2	-	3.0	-	-	-	-	0.8	0.3	-	-	36.2	99.3
This Study	0.22	55.02	28.19	6.38	1.77	0.00	-	1.05	2.48	2.50	0.00	-	-	

Table-4 Comparative Analysis of the Functional Group of the Heterogenous Catalyst

Source	Functional Group
Mangifera indica peel (Laskar <i>et al.</i> , 2020)	Carbonate, Carbonyl, Hydrocarbon, Halo compound, metal oxides
Cocoa pod husk + plantain peel (Olatundun <i>et al.</i> , 2020)	Hydroxyl, Carbonate, Metal oxides
This Study	Hydroxyl, Hydrocarbon, Halo compound, metal oxides

CONCLUSION

In this study, the following conclusions were made based on the findings:

The precursors were successfully prepared through series of unit operations and were characterized. The precursors were combined in equal ratio and calcined at a temperature of 750°C in 45mins thereby leading to its activation into a heterogenous catalyst.

The heterogenous catalyst was characterized using techniques such as FT-IR, SEM/EDX, BET, TGA and XRD. The FT-IR analysis revealed the existence of hydroxyl, hydrocarbon, and halogen compounds. The SEM/EDX evaluation examined the surface structure and elemental makeup, demonstrating a significant presence of alkali metals (potassium, sodium) and alkaline earth metals (calcium, magnesium). The BET analysis showed a pore diameter of 2.072 nm, a pore volume of 0.191 cc/g, and a surface area of 395.047 m²/g. The TGA analysis indicated thermal stability, with the optimal calcination temperature for the precursor determined to be 480°C at a shorter duration. The XRD analysis identified the presence of muscovite, indicating that the heterogeneous biocatalyst exhibited high crystallinity. A comparative analysis was done on the biocatalyst by comparing its elemental composition and functional groups with other biocatalysts; it was clear that it is appropriate for biodiesel production since it showed comparable characteristics.

CONTRIBUTION TO KNOWLEDGE

This research contributes to sustainable development by reducing waste, promoting renewable energy and supporting eco-friendly technologies. Developing heterogenous catalyst from cocoa pod husk and sawdust reduces waste and promotes sustainability.

CONFLICT INTEREST

The authors declare that they have no conflict of interest

REFERENCES

- Anaraga, S. B., Shamsudin, R., Hamzah, M. H., Sharif, S., & Dwi, S. (2024, July). Cocoa by-products: A comprehensive review on potential uses, waste management and emerging green technologies for cocoa pod husk utilization. *Heliyon*, 10(16). <https://doi.org/10.1016/j.heliyon.2024.e35537>
- Betiku, E., Pereao, O., & Ojumu, T. (2017). Two-Step Conversion of Neem (*Azadirachta indica*) Seed Oil into Fatty Methyl Esters Using a Heterogeneous Biomass-Based Catalyst: An Example of Cocoa Pod Husk. *ACS (Energy and Fuels)*, 31(16), 6182-6193. <https://doi.org/10.1021/acs.energyfuels.7b00604>
- Eldiehy, K., Daimary, N., Borah, D., Sarmah, D., Bora, U., Mandal, M., & Deka, D. (2022). Towards biodiesel sustainability: Waste sweet potato leaves as a green heterogeneous catalyst for biodiesel production using microalgal oil and waste cooking oil. *Elsevier*, 187. <https://doi.org/10.1016/j.indcrop.2022.115467>
- Etim, A., & Musonge, P. (2024). Synthesis of a Highly Efficient Mesoporous Green Catalyst from Waste Avocado Peels for Biodiesel Production from Used Cooking-Baobab Hybrid Oil. *Catalysts*, 261(14). <https://doi.org/https://doi.org/10.3390/catal14040261>
- Falowo, O. A. & Betiku, E. (2020). A noFvel heterogeneous catalyst synthesis from agrowastes mixture and application in transesterification of yellow oleander-rubber oil: optimization by Taguchi approach, *Fuel* 312, 122999
- Falowo, O. A., Oladipo, B., Taiwo, A. E., Olaiya, A. T., Oyekola, O. O & Betiku, E. (2022). Green heterogeneous base catalyst from ripe and unripe plantain peels mixture for the transesterification of waste cooking oil. *Chemical Engineering Journal Advances* 10 (2022) 100293. <https://doi.org/10.1016/j.ceja.2022.100293>
- Gronenberg, L., Marcheschi, R., & Liao, J. (2013n, June). Next generation biofuel engineering in prokaryotes. *Current Opinion in Chemical Biology*, 17(3), pp. 462-471. <https://doi.org/https://doi.org/10.1016/j.cbpa.2013.03.037>
- Kasi, G., Stalin, N., Rachtanapun, P., Jantanasakulwong, K., Halder, J., Phongthai, S., Thanakkasaranee, S. (2025, May 19). Effect of Calcination Temperatures on Crystallite Size, Particle Size, and Antimicrobial Activity of Synthesized MgO and Its Cytotoxicity. *International Journal of Molecular Science*, 26(10). <https://doi.org/https://doi.org/10.3390/ijms26104868>.

Laskar, I., Gupta, R., Chatterjee, S., Vanlalveni, C., & Rokhum, S. (2020). Taming waste: Waste *Mangifera indica* peel as a sustainable catalyst for biodiesel production at room temperature. *Elsevier*, 161, 207-220. <https://doi.org/https://doi.org/10.1016/j.renene.2020.07.061>

O'latundun, E. A., Borokini, O. O., & Betiku, E. (2020). Cocoa pod husk-plantain peel blend as a novel green heterogeneous catalyst for renewable and sustainable honne oil biodiesel synthesis: A case of biowastes-to-wealth, *Renew. Energy* 166 163-175. <https://doi.org/https://doi.org/10.1016/j.renene.2020.11.131>

Pandeeti, E. P., Veeraiah, S., & Routhu, G. D. (2019). Emerging Trends in the Industrial Production of Chemical Products by Microorganisms. In B. Viswanath (Ed.), *Recent Developments in Applied Microbiology and Biochemistry* (pp. 107-125). <https://doi.org/https://doi.org/10.1016/C2017-0-04612-8>

Patil, S. S., & Rathod, V. K. (2021). Intensification of extraction of biomolecules using three-phase partitioning. In *Three Phase Partitioning: Applications in Separation and Purification of Biological Molecules and Natural Products* (pp. 285-322). India. <https://doi.org/https://doi.org/10.1016/B978-0-12-824418-0.00009-6>

Shetty, A., Molahalli, V., Sharma, A., & Hegde, G. (2023). Biomass-derived carbon material in heterogenous catalysis: A step towards sustainable future. *Catalysts*, 13(20). <https://doi.org/https://doi.org/10.3390/catal13010020>

Sui, H., Wang, B., Chen, Z., Liu, Y., Sagoe-Crentsil, K., & Duan, W. (2024, November). Optimizing calcination for low-grade calcined kaolinite clay: Reactivity and energy consumption. *Elsevier*, 21. <https://doi.org/https://doi.org/10.1016/j.cscm.2024.e04056>

Wang, Y., Qin, Y., Liu, S., Zhao, Y., Liu, L., Zhang, Z., Qin, M. (2025, April). Mesoporous Single-Crystalline Particles as Robust and Efficient Acidic Oxygen Evolution Catalysts. *American Chemical Society*, 147(16), 13345-13355. <https://doi.org/https://doi.org/10.1021/jacs.4c18390>